The UV Albedo of Triton in Late 1999 from HST/STIS Spectra and Images.

L. A. Young, S. A. Stern (SwRI), M. W. Buie (Lowell Obs), M. D. Hicks, B. J. Burratti (JPL),
L. M. Trafton (Univ. TX at Austin), J. Stansberry (Steward Observatory)

1. Introduction

Neptune's largest satellite, Triton, has proven to be one of the most complex and fascinating bodies in the solar system, with a cryogenic atmosphere, and a morphologically complex surface (see Smith et al1989; Broadfoot et al. 1989; McEwen 1990). Triton's atmosphere is dominated by N2 gas (Broadfoot et al. 1989), with a surface pressure of ~16 µbar (Tyler et al. 1989). Voyager 2 discovered detached hazes, and active vents generating plumes kilometers into Triton's atmosphere (Smith et al.1989; Broadfoot et al. 1989). Triton's surface, at a temperature near 38 K (Tyler et al. 1989; Conrath et al. 1989; Tryka et al 1993), contains the volatile frosts N2, CO, and CH_4, as well as less volatile CO_2, coloring agents, and absorbers (e.g., Thompson and Sagan 1990; Quirico et al 1999 1999; Brown & Cruikshank 1997 and references therein). The atmosphere strongly affects the appearance of Triton's surface, through plume streaks and the sublimation/recondensation cycle.

Adding to the scientific interest in Triton, surface imagery obtained by Voyager 2 in 1989 show a distinct lack of craters; owing to this, Triton's surface is widely thought to be geologically younger and more active than almost any other planetary satellite (e.g., Smith et al. 1989; Strom et al. 1990; Stern & McKinnon 2000). The source of this geologic activity is not known (e.g., McKinnon et al. 2000), but it is known that volatile transport drives additional change on Triton's surface. The volatile transport is driven by Triton's orbit and Neptune's obliquity, which together cause Triton to experience extreme seasonal variations in subsolar latitude (Harris 1984). Because of the exponentially sensitive temperature dependence of the volatility of the frosts, this leads to dramatic seasonal effects, including widescale frost migration and dramatic changes in atmospheric pressure (e.g., Trafton 1984; Spencer & Moore 1992). As volatile frosts migrate from sunlit to darker areas on Triton, they likely expose underlying layers and modify the optical properties of the surface (e.g., Trafton 1984; Spencer 1990), affecting Triton's albedo, color, and spectral signature. Because of Triton's high bond albedo (*A*=pq=0.89; McEwan 1990), the surface energy balance is extremely sensitive to these photometric changes.
Planetary astronomers have expected detect observable effects of these predicted changes as Triton approaches a seasonally-driven, "major summer" around the start of the 21st century. And indeed, evidence is now mounting that Triton is undergoing a significant period of global seasonal change. One key indicator is the Elliot et al. (1998, 2000a, 2000b) reports, based on stellar occultations, that Triton's atmospheric pressure has been increasing since 1989 (with most of the increase occurring in the last 5 years), implying that the surface has warmed. Another key indicator is the recently-reported reddening in Triton's color detected by Buratti et al. (1994, 1999).

In addition to these secular changes that are likely to be forced by the seasonal major summer, transient changes in Triton's color and albedo have also been observed (Buratti et al. 1999); these changes induce temporary but dramatic reddenings of Triton's visible spectral slope, during which the ratio of U to V albedo changes by factors of 2. Because of the sparsity of existing observations, it is unknown how quickly or frequently these changes occur.

Based on the increasing pace and diversity of changes being observed on Triton in the mid-to-late 1990s, and the fact that the UV is usually more sensitive to contrast changes on icy surfaces than are other spectral regions (e.g., Stern, Buie, & Trafton 1997), we conducted a first look for changes in the UV photometric appearance of Triton using HST's STIS spectrometer in HST Cycle 8, in program 8218. This effort consisted of a program of 3 mid-UV spectroscopic and concurrent 3 mid-UV imaging observation sets in Aug/Sept 1999, which we report on here. In what follows we describe these observations, present reductions of the data gathered, and then compare the results we obtained to previous observations, including other mid-UV HST observations obtained in 1992/1993 (Stern et al. 1995), Voyager 2 UV photometry (Lane et al. 1989), and groundbased work obtained by others in 1999 (Buratti & Hicks 2000).

Preprint signup

2. Observation and Reduction

Table 1: Dates of the three visits of program 8218

Visit	Date	Triton Central Meridian Longitude
1	1999 Aug 28	8°
2	1999 Sep 11	249°
3	1999 Sep 13	130°

Triton was observed using the STIS instrument on the Hubble Space Telescope (HST) in late 1999 as part of program 8218 ("Exploring Triton in the act of Global Change").

Table 2: Exposures taken during each visit of program 8218

Data product	Detector	Grating/Filter	Wavelength	Exp. Time
1 spectrum	MAMA	G230 L	1570-3180Å	1153 s/spectrum
4 dithered images	CCD	F28x50OII	3737 Å	50 s/image
4 dithered images	MAMA	F25CN270	2710 Å	150 s/image

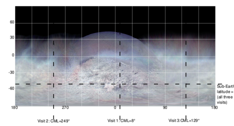

3. Photometry

For all images, countrates are converted to geometric albedo using:

$$p(\lambda) = \frac{D^2\Delta^2}{R^2}\frac{C_{Triton}(\lambda)}{C_{Solar}(\lambda)}f_\alpha \qquad (1)$$

where D and Δ are the heliocentric and geocentric distances, R is the radius of the target, and f_α is the correction for nonzero solar phase angle. C_{Triton} is the observed countrate from Triton. We use the HST-supplied IRAF routine synphot to calculate C_{Solar}, the countrate for a target with the same flux as the sun. We describe the reduction for each of the two filters below.

To calculate f_α we use the linear phase coefficient of $\beta = 0.011$ mag/deg (Lane et al. 1989). For the UV flux of the sun, we used the SUSIM UARS SOLSTICE solar irradiance spectra for 1999 Aug 31, 1999 Sep 14, and 1999 Sep 17 (Woods et al. 1996; Tom Woods, private communication, 2000). We used postdated spectra to account for the modulation in the solar spectrum due to the sun's 27-day rotation, since Triton "sees" a different face of the sun than an earth-orbiting spacecraft.

3737 Å Images (CCD)

Fig. 1: Throughput for 3737 Å filter

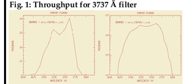

We observed with the F28x50OII filter, which has a central wavelength of 3737.3 Å, and a FWHM of 57.0 Å.

Fig. 2: Typical CCD image and 0.25 arcsec aperture

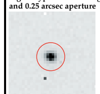

The pixel scale for these images was 50 mas/pixel. We performed standard aperture photometry, with an aperture radius of 0.25 arcsec (5 pixels), and a background annulus which ranged from 0.5 to 2.5 arcsec (10 to 50 pixels). For point sources, the fraction of encircled energy for a 0.25 arcsec aperture through this filter is 92% (STIS Instrument Handbook, v. 3.0, chapter 14). Convolution by Triton's disk leaves the encircled energy essentially unchanged, even assuming no limb darkening.

2710 Å Images (MAMA)

Fig. 3: Throughput for 2710 Å filter

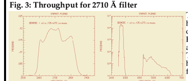

The F25CN270 filter has a central wavelength of 2710.6 Å and a FWHM of 160.6 Å, and a redleak; counts from Triton's visible photons have to be subtracted from C_{Triton} before applying Eq. 1.

To correct for the redleak in the F25CN270 filter, we calculated the expected flux from Triton from 3250 to 7000 Å, using a solar spectrum obtained FTS from 2960 to 13000 Å and tabulated on a grid of roughly 0.005 Å (Kurucz et al 1984), an albedo at the wavelengths sensitive to the redleak of ~0.7, and the nominal V phase coefficient of 0.027 mag/deg (Goguen et al 1989). The fluxes were then converted to a countrate using the synphot IRAF routine, provided by the Space Telescope Science Institute. The redleak contributed 12-15% of the total observed counts, varying with visit. The uncertainty in the average albedo at the wavelength of the redleak leads to an uncertainty of 0.5% in the redleak-corrected countrate.

Fig. 4: Typical MAMA image and 0.24 arcsec aperture

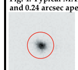

The pixel scale for these images was 24 mas/pixel. We performed standard aperture photometry, with an aperture radius of 0.24 arcsec (10 pixels), and a background annulus which ranged from 0.36 to 1.8 arcsec (15 to 75 pixels). For point sources, the fraction of encircled energies for a 0.24 arcsec aperture through this filter is 85%. As before, convolution by Triton's disk leaves the encircled energy essentially unchanged, even assuming no limb darkening.

4. Spectroscopy

The spectra were taken with the G230L grating and the 52×0.5 arcsec slit, with a nominal spectral range of 1570–3180 Å and a nominal dispersion of 1.58 Å/pixel.

Fig. 5: Flux from Triton and the Sun

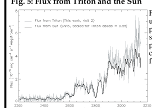

For each of the three spectra, we use the calibrated data products produced by the version 2.0 of standard calstis pipeline, which produces files of wavelength-calibrated fluxes and errors (the *x1d* files).

However, we found that observed albedos at 2710 Å derived from the spectra were low relative to the MAMA images, by a factor of 0.05, 0.24, and 0.30 for visits 1, 2, and 3 respectively. This is due to miscentering of the target, a diagnosis that is confirmed by the observed shift in Triton's wavelength scale relative to the solar spectrum. Fortunately, we can use the MAMA images to normalize the spectra at 2710 Å. The only remaining question is the wavelength dependence of the out-of-center throughput.

Fig. 6: Calculating out-of-center slit throughput

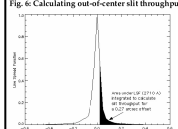

We calculate the out-of-center throughput as a function of offset by integrating the LSF over an off-center 0.5 arcsec region, relative to the integral of a centered region. We used observations of spectra to measure the line-spread function (LSF) in the cross-dispersion direction (taken as part of the calibration proposal 7721). This allows us to calculate both the offset and the wavelength dependence of the out-of-center slit throughput.

Fig. 7: Accuracy of slit-throughput correction

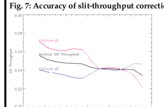

The wavelength dependence of the slit throughput depends on the direction in which we offset our synthetic slit. We use this difference to estimate of the error in the wavelength dependence of the slit throughput, based on the difference between the LSF in the dispersion and cross-dispersion direction. We find that the throughput is nearly constant longward of 2710 Å, with small relative errors (~1%). From 2200 to 2550 Å, the shape of the slit throughput is also independent of the direction of offset at ~1%. However, uncertainty in the slit throughput leads to a 11% uncertainty in the flux between 2200-2500 Å relative to 2710-3200 Å.

5. Results

Fig. 8: Triton UV albedos, 1989-1999

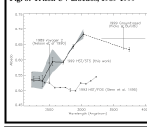

The mean UV albedos of Triton from 3 dates in Aug. and Sep. 1999 from HST/STIS are plotted with diamonds and thick lines in Fig. 8. The dashed line connects the spectral measurements (2200-3000 Å) with the CCD imaging measurement (3737 Å). The MAMA imaging measurement is identical with the spectral measurement at 2710 Å, since the MAMA images were used to rescale the spectra. Error bars indicate random errors only. The uncertainty in the wavelength dependence of the slit throughput is indicated by the gray region.

6. Conclusions

1. Triton has brightened by 16-30% from 1993 to 1999 at 2630-3200 Å.

Comparing the mid-UV (2500–3200 Å) spectroscopy obtained by HST/STIS in Aug–Sep 1999 to the mid-UV (2200–3200 Å) spectroscopy obtained by HST/FOS in Sep 1993, we find that Triton's mean geometric albedo increased significantly, by 16±4% at 2550Å and 30±7% at 3110Å. Between 2200 and 2470 Å, no change in geometric albedo was detected at the 12% level.

Table 3: Triton brightening, 1993 to 1999

Wavelength range	Ratio of albedo, 1999 (STIS)/1993 (FOS)
2150-2470 Å	0.99 ± 0.11
2470-2630 Å	1.15 ± 0.15
2630-2790 Å	1.16 ± 0.04
2790-2950 Å	1.28 ± 0.05
2960-3110 Å	1.30 ± 0.07

Note: Errors in Table 3 are dominated by the uncertainty in the overall scaling, namely: uncertainty in the slit throughput (2150-2630 Å and 2960-3110 Å) or the photometric stability of STIS or FOS (2630-2960 Å).

The 2700 Å albedo obtained by HST/STIS in Aug-Sep 1999 (0.56±0.06) is consistent with Voyager 2/PPS UV photometry at this same wavelength (0.59±0.06; Nelson et al. 1990).

The combination of the HST/STIS data and the groundbased U albedo obtained on 15 Aug 1999 (Hicks & Buratti 2000) indicate that Triton
(i) was not in a reddened state from 18 August to 13 September 1999, and (ii) was likely photometrically stable at the few percent level during this timeframe.

2. The slope of Triton's UV spectrum (2200-3200 Å) has reddened from 1993 to 1999.

Fig. 9: Change in Triton's UV spectrum, 1993-1999

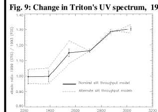

Between 1993 and 1999, Triton's UV spectrum has become redder between 2200 and 3200 Å. Furthermore, there is a suggestion of an absorption edge near 2500 Å. Error bars indicate random errors only. The uncertainty in the wavelength dependence of the slit throughput is indicated by dashed lines.

3. Triton's spatial contrast appears lower in 1999 than in 1989 or 1993.

Fig. 10: Triton lightcurve amplitudes

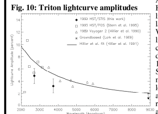

As seen with Voyager and HST/FOS, Triton's UV rotational lightcurve amplitude in 1999 is larger at 2710 than at 3737 Å. While the 1993 rotational lightcurve amplitude was consistent with the Voyager-derived model of Hillier et al. 1991 (Stern et al. 1995), the 1999 STIS data indicate that Triton's mid-UV rotational lightcurve is lower, by 32% at 2710 Å and 37% at 3737 Å. The sparsity of the rotational sampling probably accounts for only 12% of this difference. Note that the sub-observer latitude observed from HST in 1999 (-50°) is similar to that observed by Voyager 2 in 1989 for most of the images used by Hillier et al. 1991 (–49 to –55°).

The results we have reported here demonstrate that Triton's UV photometric properties have changed in several key respects between 1993 and 1999. We interpret this as a consequence of seasonal and/or transient changes, most likely due to volatile transport, perhaps combined with a change in the photometric properties of Triton's hazes. As with visible-wavelength photometry and occultation-based probes of Triton's atmospheric structure, more frequent and rotationally-denser measurements are required in the UV.